Identification of Melatonin-Regulated Genes in the Ovine Pituitary Pars Tuberalis, a Target Site for Seasonal Hormone Control

Endocrinology. First published ahead of print July 31, 2008 as doi:10.1210/en.2008-0834

Identification of melatonin-regulated genes in the ovine pituitary *pars tuberalis*, a target site for seasonal hormone control.

Sandrine M. Dupré[1], Dave W. Burt[2], Richard Talbot[2], Alison Downing[2], Daphne Mouzaki[2], David Waddington[2], Benoit Malpaux[3], Julian RE Davis[1], Gerald A. Lincoln[4] and Andrew SI. Loudon[1*]

[1]University of Manchester, Faculty of Life Sciences and Faculty of Medical and Human Sciences, Manchester, UK; [2]University of Edinburgh, Roslin Institute, Midlothian, UK; [3]Physiologie de la Reproduction et des Comportements, UMR INRA-CNRS-University of Tours-Haras Nationaux, 37380 Nouzilly, France. [4]University of Edinburgh, Centre for Reproductive Biology, QMRI, Little France Crescent, Edinburgh, UK

Disclosure statement: The authors have nothing to disclose

*Correspondence and reprint request
Andrew Loudon
Faculty of Life Sciences
3.614 Stopford Building
Oxford Road
Manchester M13 9PT, UK
Andrew.loudon@manchester.ac.uk

Abbreviated title: Melatonin-regulated genes in the sheep Pituitary *pars tuberalis*

Key words: Photoperiod, Pituitary, Pars tuberalis, Melatonin, circadian, *NeuroD1*, *Nampt*, *Hif1α*, *Cry1*.

Funding: This work was supported by the Biotechnology and Biological Sciences Research Council, UK (grant to AL and JRED).

ABSTRACT: The *pars tuberalis* (PT) of the pituitary gland expresses a high density of melatonin (MEL) receptors and is believed to regulate seasonal physiology by decoding changes in nocturnal melatonin secretion. Circadian clock genes are known to be expressed in the PT in response to the decline (*Per1*) and onset (*Cry1*) of MEL secretion, but to date little is known of other molecular changes in this key MEL target site. To identify transcriptional pathways that may be involved in the diurnal and photoperiod-transduction mechanism, we performed a whole genome transcriptome analysis using PT RNA isolated from sheep culled at three time points over the 24h cycle under either long or short photoperiods. Our results reveal 153 transcripts where expression differs between photoperiods at the light/dark transition and 54 transcripts where expression level was more globally altered by photoperiod (all time points combined). *Cry1* induction at night was associated with up-regulation of genes coding for *NeuroD*1 (Neurogenic differentiation factor 1), *Pbef/Nampt*, (nicotinamide phosphoribosyltransferase), *Hif1*α (hypoxia-inducible factor-1alpha) and *Kcnq*5 (K^+ channel) and down-regulation of *Rorβ*, a key clock gene regulator. Using *in situ* hybridization, we confirmed day-night differences in expression for *Pbef/Nampt*, *NeuroD1* and *Rorβ* in the PT. Treatment of sheep with MEL increased PT expression for *Cry1, Pbef/ Nampt, NeuroD1* and *Hif1α*, but not *Kcnq5*. Our data thus reveal a cluster of *Cry1* associated genes which are acutely responsive to MEL and novel transcriptional pathways involved in MEL action in the PT.

Seasonally breeding animals have to anticipate environmental events in order to optimize their survival and reproductive success. The annual photoperiod cycle provides a critical environmental signal, which entrains seasonal physiology. Nocturnal secretion of the pineal hormone melatonin reflects these seasonal changes in photoperiod and thereby provides the brain with an internal hormonal representation of external photoperiod changes. Seasonal cycles in melatonin modulates multiple physiological systems including reproduction, food intake, adiposity, body temperature regulation and many neuroendocrine pathways (reviewed in (1)). One prominent seasonal neuroendocrine output is the release of prolactin. This axis is exquisitely sensitive to photoperiod in all seasonally breeding mammals, with marked activation of prolactin secretion by long summer-like photoperiods (2).

The *pars distalis* (PD) of the pituitary is thought to be regulated by paracrine signals from the *pars tuberalis* (PT), a melatonin receptor-rich tissue lying on the ventral surface of the median eminence (ME), and creating an interface between the hypothalamus and the PD (3). PT cells are known to secrete an un-characterised low molecular weight peptide(s) (termed "tuberalin"), which is capable of eliciting prolactin secretion from distal lactotroph cells in culture (4-7). These studies have led to the proposal that melatonin acts on PT cells to elicit a local paracrine secretion of a prolactin-releasing peptide. *In vitro* studies of seasonal hamster tissue has revealed that the activity of this secretagogue is under photoperiodic control, with higher levels of activity observed in PT tissue derived from long photoperiod (LP) compared to short photoperiod (SP)-housed animals (6). Surgically hypothalamo-pituitary disconnected (HPD) sheep, in which the PT has been disconnected from the hypothalamus, retain both robust photoperiodically-driven cycles of prolactin secretion and sensitivity to melatonin (8). Further, HPD sheep are also capable of generating long-term circannual rhythms of prolactin secretion when maintained in unchanging photoperiod conditions. This result suggests that this tissue may operate both as a seasonal calendar, responding to seasonal changes in the melatonin signal, and as a circannual oscillator (9). Collectively, these studies support a hypothesis that melatonin regulation of the seasonal prolactin axis is dependent upon melatonin acting on PT cells without input from the hypothalamic or other neural structures, and regulating seasonal prolactin secretion *via* a direct intra-pituitary paracrine mechanism.

Here, we investigated seasonal transcriptional changes occurring in the PT, using RNA extracted from sheep kept under SP or LP and

collected at three time-points over the light/dark cycle. For whole genome transcriptome analysis sheep RNAs were cross-hybridised against a bovine 15,000 gene cDNA microarray, allowing comparison of relative expression at each of the three time points for SP and LP housed individuals. Of the 15,000 probes spotted on the array, 54 transcripts exhibited a significant, photoperiod-dependent alteration in expression, including *Prnp*, encoding the prion protein which was strongly up-regulated on SP. 153 transcripts exhibited significantly altered expression associated with the light/dark transition and onset of melatonin secretion on SP. Among these, the circadian clock gene *Cry1* was the most strongly displaced of all genes on the array, with strong up-regulation at the time of melatonin rise on SP. In addition to *Cry1*, we identified a small cluster of genes at this time point, including *Kcnq*5, *Pbef/Nampt* involved in insulin regulation, energy metabolism sensing and adipose tissue physiology, *NeuroD*1 and the hypoxia inducible factor (*Hif1α*), both of which act as bHLH transcription factors. We validated the arrays by Q-PCR for two of these transcripts (*NeuroD1* and *Pbef/Nampt*) and confirmed differential expression at early night in SP. All 5 transcripts showed strong expression in the PT using *in situ* hybridization. In order to determine whether these *Cry1*-associated transcripts were also directly responsive to melatonin, we tested acute responses of these genes following melatonin treatment in sheep. Four genes (*Cry1*, *NeuroD1*, *Pbef/Nampt* and *Hif1α*) were immediately and strongly induced by melatonin treatment.

Our study identifies new transcriptional pathways and candidate genes regulated by photoperiod and/or at specific phases of the light/dark cycle in the sheep PT, and also identifies novel genes which are acutely regulated by melatonin.

Materials and Methods

Array experiments and collection of tissue for validation of outcomes

Animals and experimental design: Animals were castrated as lambs on the farm as part of normal agricultural practice and use of this castrate model allowed studies of seasonal changes in gene expression without the complication of altered background levels of sex steroids.

Array experiments: For comparison using arrays, 40 male Black-face sheep were housed indoors from mid-winter (January 13) under artificial long photoperiod (LP =16 hours light: 8 hours dark). At Week 14, 20 animals were killed at three different time points: Zeitgeber time (ZT) 4 (n=7), ZT12 (n=7) and ZT20 (n=6), where ZT0 by convention represents the transition from light to dark of a 24h cycle. Two weeks later, the remaining cohort were switched to artificial short photoperiods (SP = 8 hours light: 16 hours dark) for 10 weeks and then killed at the same time points at Week 26. Dim red background lighting was provided throughout (<5 lux). By this means, the LP cohort were collected at two time points in the light (ZT4 and 12) and one in the dark (ZT20) while the SP group were culled at one time point in the light (ZT4) and two in the dark (ZT12, 20). The experimental design is outlined in Fig. 1. This allowed subsequent comparisons between photoperiods and also at time of lights off/melatonin rise for LP and SP housed animals (see below). Animals used in the array experiment were blood-sampled for prolactin determination (10 animals per photoperiod group) at twice weekly intervals; plasma was separated by centrifugation and stored at -20^{O}C until assayed. Prolactin samples were assayed in duplicate as previously described (10). Intra and inter assay coefficients of variance were <10%.

Collection of tissue for validation of array outcomes: To provide tissues for the localization of candidate genes identified on the arrays, 12 intact male Soay sheep were kept under SP for 6 weeks, and 6 were culled at ZT3 and 6 at ZT11 on SP's (lights off at ZT8).
For the array studies, brains were rapidly removed and the *pars tuberalis* (PT) was removed by microdissection, snapped frozen on dry ice and kept at -80°C until RNA extraction. For the other *in situ* hybridization determinations, brains were removed and hypothalamic blocks including the PT were

isolated by dissection and kept at -80°C until cryostat sectioning. All animals were killed by overdose of sodium pentobarbital. During the dark phase there was no use of accessory lighting and after death the animals head was covered prior to removal of the brain. All experiments were undertaken in accordance with the Home Office Animals (Scientific Procedures) Act (1986), UK, under a Project License held by GAL.

Animals used for melatonin treatment

The experimental procedure reported in this study was carried out in accordance with the Authorization 37801 for Animal Experimentation and Surgery from the French Ministry of Agriculture. 24 adult intact female Ile de France sheep were used in this experiment. They were reared outdoors at Nouzilly, INRA, France and moved to an open indoor shed exposed to natural photoperiods (14.5h light: 9.5h dark) two weeks before the study (April 15). On May 2nd, the animals were exposed to continuous light over the entire nocturnal period in order to suppress natural melatonin production. At 07:30 the following day 12 animals were treated with two subcutaneous melatonin implants (Mélovine®, CEVA Animal Health, Libourne, France (11)) in the ear and the remainder received no implant, but had their ear punctured identically. The animals (4 per group) were subsequently culled at +1h30min, +3h30 min and +6h30 min for collection of PT and hypothalamic tissue. All animals were blood sampled 30 min after implant insertion, and again just prior to culling for determination of melatonin concentrations in blood plasma using a standardized radioimmunoassay (12). All samples were included in the same assay and the intra-assay CV was 2.7%.

Ovine cDNA

Ovine PT RNA (1.5µg) was reverse transcribed to undertake 3'- and 5'-RACE PCR (BD SMART RACE cDNA amplification, BD biosciences, Oxford, UK) to obtain ovine cDNA sequences for *NeuroD1* and *Pbef/Nampt*, following the manufacturer recommendations. Gene Specific Primers (GSPs) and Nested Gene Specific Primers (NGSPs) were designed according to Mouse *NeuroD1* mRNA sequence (NM 010894) (GSP1:5'-CAG TCA CTG TAC GCA CAG TGG ATT CG-3'; NGSP1:5'-GGA ATA GTG AAC TGA CGT GCC-3'; GSP2:5'-GAG CGA GTC ATG AGT GCC CAG C-3' ; NGSP2: 5'-GGC ACG TCA GTT TCA CTA TTC C-3') and Human *Pbef1* mRNA sequence (NM 005746) (GSP1:5'-GCC TAA TGA TGT GCT GCT TCC AGT TC-3' ; NGSP1:5'-TCT TCA CCC CAT ATT TTC TCA CAC GC-3'). Amplified product were then ligated into pGEM-T Easy (Promega, Southampton, UK) and selected clones were sequenced using Big Dye Terminator v1.1 Cycle Sequencing kits (Amersham, Piscataway, NJ, USA, following the manufacturer protocol) by the DNA sequencing service at the University of Manchester. Sequences obtained for *NeuroD1* and *Pbef* were submitted to the Genebank database (Accession numbers DQ_82274, DQ_822275).

A 350 to 450 bp cDNA fragment was sub-cloned in pGEM-T easy for *NeuroD1* and *Pbef*, using 5'-ACT GCC TTT GGT AGA AAC AGG G-3' or 5'-AGA TCC AAG AAG CCA AAG AGG-3' respectively as forward primer and 5'-GCT AAG GCA ACC CCA ACA AC-3' or 5'-GAA GTT AAC CAA ATG AGC AGA TG respectively as reverse primer. These clones were used to prepare standards for Q-PCR experiments and riboprobes for *in situ* hybridizations.

Ovine PT tRNA was reverse transcribed and used directly as template to clone a fragment of 350 to 450bp in pGEMT-easy using the following primers : 5'-CCA TGG TGA CCA CGG GT-3'and 5'-AGC TAA GAG CAT CGA GGG G-3' for *18S* (AF_176811); 5'-CTG CAC CAC CAA CTG CTT AG-3 ' and 5'-TG TCG TAC CAG GAA ATG AGC-3' for *Gapdh* (U_94889); 5'-CCC ACT CAA ATG CAA GAA CCT CC-3' and 5' - CGC TTT CTC TGA GCA TTC TGC A - 3' for *Hif1α* (NM_174339); 5'–TGG TCT ACG CGC ACA GCA AG-3' and 5'-CTG CAG GTG TGC AAG GCC TT-3' for *Kcnq5* (XM_864552). Sequences obtained for *Hif1α* and *Kcnq5* were submitted to the Genebank database (Accession numbers EU_706449 and EU_706550). Clones for *18S* and *Gapdh* were used to obtain Q-PCR standards, those obtained for *Hif1α* and *Kcnq5*

were used to obtain riboprobes for *in situ* hybridizations.

Quantitative PCR and in situ hybridization

2µg of each RNA sample used in the microarray experiments was reverse transcribed for Q-PCR validation. Genomic DNA was removed using 1 unit of RQ1 RNase-free DNase (Promega) for 30 min at 37°C, the reaction was stopped by adding 1µl of the DNase stop solution (Promega) and incubating the samples 10 min at 65°C and the 1 min on ice. Samples were then processed for cDNA conversion in a final volume of 20µl containing 0.5µM oligo-dT (5'-TTT TGT ACA AGC T_{23}-3'), 500µM each dNTP, 1X first-strand buffer, 10µM DTT and 10U SuperScript™ Reverse Transcriptase II (Invitrogen, Paisley, UK). The samples were incubated for 1 hour at 42°C and reverse transcriptase was inactivated by heating at 70°C for 15 min. Negative controls without enzyme were done in parallel. For quantification, standards were cloned as described above and used as template for PCR reactions with the cloning primers and usual PCR methods. Each samples was processed for Q-PCR as duplicates; reactions were done in 25µl final contained 5µl cDNA (or DEPC-treated water for negative control, or standard samples), 100nM TaqMan probe (Eurogentec, Southampton, UK), forward and reverse primers at 300nM each, and 1x qPCR MasterMix and using the following cycling conditions : 2 min at 50°C, 10 min at 95°C and 40 cycles of 95°C for 15 sec and 60°C for 1 min. Primers and TaqMan probes were designed using the Primer Express 2.00 software, sequences are shown in Table S1. Data were obtained through the ABI Prism 7000 SDS software (version 1.1, Applied Biosystems, Warrington, UK). Values are shown as relative units with the ZT4 value in LP set at 1.

Radiolabelled sense and anti-sense ovine riboprobes for *Cry1, Per1*, *NeuroD1*, *Pbef/Nampt*, *Rorβ*, *Hif1α* and *Kcnq5* (cloned as described above) were produced using a T7 or Sp6 polymerase as appropriate on linearised templates in the presence of ^{33}P-UTP (MP Radiochemicals, USA)**.** The following *in situ* hybridisation procedure was previously described by (13)**.** Briefly, probes were hybridized overnight at 60°C on coronal or sagital hypothalamic sheep brains cryostat sections (20µm thick for the validation of the array outcome and 18µm for the melatonin experiment). Hybridization signals were visualised on autoradiographic films (Kodak Biomax MR Films, Kodak, USA) after one week exposure at -80°C. Signal intensity was quantified by densitometry analysis of autoradiographs using the image-Pro Plus 6.0 software (Media Cybernetics, Inc., Marlow, UK) on the coronal sections (4 animals per group except the Ctl 1h30 (n=3) in Fig.6). Relative optical density in the PT was then calculated for each group.

Analysis of differentially expressed gene sets

The R/Bioconductor analysis, described in the supplementary information, identified genes differentially expressed between LP/SP days either at ZT4, ZT12 or ZT20. In addition, a filter of greater than 1.3-fold difference in gene expression was used to limit the number of genes to the most biological relevant. Up-regulated genes show expression on LP > SP days, and down-regulated genes expression on LP < SP days. Since cDNA arrays yield relative ratio-based data rather than absolute values, for purposes of subsequent descriptions, all gene changes are described with reference to long-day mRNA values (i.e. described as up or down-regulated on long photoperiods). The design of the experiment allowed three gene expression patterns to be analysed (Table 1), namely photoperiodically regulated, SP early night regulated, and SP late night regulated.

Ontologizer (14); www.charite.de/ch/medgen/) was used to analyse differentially expressed genes for overrepresentation of Gene Ontology (GO) terms. This parent–child procedure measures overrepresentation conditional on annotations to the parent of any term, whereas previous approaches measure overrepresentation of each term in isolation. Definitions of GO terms (version 5.623) and gene associations were downloaded from the Gene Ontology website (15); www.geneontology.org). Human orthologs (Uniprot accessions) of cattle proteins were used for GO term analyses. The associations of GO terms with Uniprot accessions of human proteins were provided by GOA (version 1.75) (16). The

overrepresentation of GO terms for proteins in a set of differentially expressed genes was compared to a reference set of proteins, which contains all the genes expressed on the 15K cattle cDNA array. The parent–child-union option was used, which is less conservative than the parent–child-intersection method. The P-values were adjusted using Westfall–Young single-step multiple testing correction (17).

Pathway-Express (18); http://vortex.cs.wayne.edu/) was used to detect significant associations between differentially expressed genes and known pathways. In this method an impact factor is calculated for each pathway incorporating parameters such as the normalized fold change of the differentially expressed genes, the statistical significance of the set of pathway genes, and the topology of the signaling pathway. The impact factor corresponds to the negative logarithm of the global probability of having both a statistically significant number of differentially expressed genes and a large perturbation in the given pathway. The input to *Pathway-Express* was a set of differentially expressed genes and their fold changes, using the gene symbols of human orthologs of cattle genes. These gene sets were compared to the reference chip, which contains all the gene symbols expressed on the 15K cattle cDNA array.

Potential transcription factor binding sites (TFBS's) were predicted using *Match*/*F-Match* (19) as overrepresented sites in cattle promoter sequences for a set of co-regulated genes. A Perl script takes as input a set of co-regulated genes ("positive set") and a set of genes not affected by the treatment ("negative set", limited to 2000 sequences) to extract cattle promoter sequences for further analysis. These promoter sequences were downloaded using Biomart from Ensembl (version 48) as the 5-kb flanking regions of all known cattle genes. *Match* was used to detect potential TFBS's using the positional weight matrices (PWM's) from the *Transfac* database (version 12.1; a library of 846 PWM's for vertebrate transcription factors (TF's)) constructed from collections of known binding sites for given TF or TF family. A built-in matrix profile with cut-off values adjusted to minimize the sum of false positive and false negative errors (vertebrate_non_redundant_minFP) was used in the detection of TFBS's. *F-Match* was then used with default parameters to detect overrepresented TFBS's. Raw probability values were extracted and used as input to *Qvalue* (20) to calculate false discovery rates (FDR).

General statistical analysis

Results are shown as means +/- SEM. After ANOVA analysis the Bonferroni test was applied to analyze differences between groups. Differences were considered significant at $P<0.05$.

Results

Photoperiod response in the animals used in the array analysis

Plasma prolactin concentrations were approximately 50-fold higher in the sheep culled across the three time points (ZT4, ZT12 and ZT20) under LP compared to the cohort culled under SP (Fig. 1). Thus the PT tissues used in the array analysis derived from animals in seasonally distinct physiological states

Gene transcriptome analysis of the ovine PT

The use of a bovine cDNA microarray relied on cross-species hybridisation between two closely related ungulates with ~97% sequence identity (21). The nature of the array comparison did not permit absolute values for altered expression to be defined since LP and SP samples were co-hybridized to the array. Thus, a transcript may appear as being up-regulated on LP, but equally the same outcome could occur if it were strongly suppressed by SP. By convention, we describe our results below in terms of relative expression in LP-housed sheep, so that transcripts exhibiting relatively greater expression in LP-derived samples are defined as being relatively up-regulated. Single channel analysis revealed that ~55% of the transcripts on the array were expressed in the sheep PT. The design of the experiment allowed three gene expression patterns to be analysed, namely genes exhibiting altered expression at all 3 time points (designated as "photoperiodically" regulated), genes exhibiting altered expression at ZT12 (designated SP early night) but not at ZT4 and

genes showing altered expression at ZT20 only (designated SP late night; Table 1).

Photoperiodic genes

Of the transcripts exhibiting significantly altered expression at all three time points a total of 36 transcripts were relatively up-regulated and 18 down-regulated (Table S2). These included up-regulation of a CREB-regulated transcription co-activator 1 gene (*CRTC1*), represented by two different probes both of which were significantly displaced on the array, and a methyl transferase gene (PMRT5). The gene encoding the prion protein (*PRNP*) was the most strongly displaced transcript in the LP-repressed cluster. The *Pathway-Express* analysis revealed over-representation of 15 pathways including olfactory transduction, MAPK and PPAR signalling pathways in the LP repressed gene set (Table 2). No significant over represented pathway was found in the LP induced set. *Ontologizer* analysis revealed significant over-representation of GO terms for carbohydrate and lipopolysaccharide processes for LP-repressed genes (Fig. S2). There was no detectable significant over-representation of GO terms in the LP induced group of genes. Analysis of putative transcription factor binding sites within each gene set included sites for homeobox, paired homeobox, bZIP and forkhead transcription factors (Table 3).

Genes changing at ZT12 (SP early night)

A total of 147 transcripts exhibited altered expression at ZT12; with 28 up-regulated and 125 down-regulated at this time point (Table S3). In the later group, the focal gene *Cry1* exhibited the greatest differential expression for any gene on the array (3.38 fold increase on SP). The activation of *Cry1* predictably occurred when ZT12 coincided with darkness under SP and light under LP. Genes exhibiting gene expression patterns similar to *Cry1* included a general transcription factor (*Gtf2a1*), the voltage-gated potassium channel *Kcnq5*, *NeuroD1* (an E-box regulated bHLH transcription factor), *Pbef (Visfatin/Nampt)* (a key regulator of the NAD/NADH salvage pathway) and the hypoxia-induced transcription factor 1 alpha (*Hif1α*, a close relative of the circadian clock gene *Bmal1*) (Table S3; Fig. 2).

Both *Hif1α* and *NeuroD1* were represented twice on the array by different regions of the cDNA, and both clones exhibited significant and similar magnitude changes, providing additional validation. Expression of *MEF2A*, a transcription factor, was also increased in SP at ZT12, consistent with a subsequent analysis identifying over represented transcription factor binding sites (see below). SP early night repressed genes (28 transcripts), included two genes involved in circadian regulation (the kinase *GSK3β* and the nuclear hormone receptor *Rorβ*). Analysis of over-representation of pathways within each gene set included pathways involved in cytokine - cytokine receptor interaction (over-represented in the SP early night (ZT12) repressed gene set) and pathways involved in circadian rhythm (over-represented in the SP early night induced gene set; Table 2). *Ontologizer* analysis revealed significant over-representation of GO terms for immune function for SP early night repressed genes (Fig. S2). There was no significant over-representation for genes up-regulated on SP's at ZT12. Analysis of putative transcription factor binding sites within each gene set included sites for bHLH-ZIP, bZIP, forkhead and paired homeobox factors for genes down-regulated at ZT12 on SP's, and bZIP, forkhead, paired homeobox, POU and MADS (represented by MEF2, myocyte-specific enhancer factor) for the SP early night induced gene set (Table 3).

Genes changing at ZT20 (SP late night)

Genes showing significant changes at ZT20 are listed in Table S4. A total of 11 transcripts were significantly up-regulated on LP at this time point (SP late night repressed), and 35 down-regulated (SP late night induced). The circadian clock gene *Bmal1 (ARNTL)* was one of the most strongly down-regulated genes (SP-late night induced), and was co-expressed with the IgG receptor precursor *FCGRT*, a glutamate/aspartate transporter (*SLC1A3*) and *QK1*, an RNA-binding protein. Analysis of over-representation of pathways included ErbB and Notch signaling pathways, circadian rhythm and olfactory transduction in the SP late night induced gene set (Table 2) while no significant over-represented pathways was found in the

other gene set. GO term enrichment within this SP late-night induced genes included genes involved in oxydoreductase activity and organelle and endoplasmic reticulum membrane.

Identification of a Cry1-associated co-expression gene cluster

The distribution of relative expression changes for ZT12 vs. ZT4 (dark vs. light) and ZT12 vs. ZT20 (early night vs. late night) under SP is shown in Fig. 2. At both time comparisons, the target gene *Cry1* was the most strongly displaced gene of the 15K transcripts detected using the array. For comparison, *NeuroD1* and *c9orf77* (both represented by two transcripts on the array) and *Pbef /Nampt* and *Gtf2a1* are also significantly displaced with strong down-regulation at ZT12 and closely associated with the *Cry1* cluster. For subsequent analyses we selected *Pbef /Nampt*, *NeuroD1*, to confirm time-of-day changes in expression and regulation in the PT, and also *Rorβ*, (significantly up-regulated at ZT12 on LP's) as an example of a gene expressed at an opposite phase.

Q-PCR and in situ hybridization comparisons

The regulation of *NeuroD1* and *Pbef/Nampt* mRNA in the PT was confirmed using quantitative PCR of PT tissue RNA (Fig. 3). In confirmation of the array data, both *NeuroD1* and *Pbef* were significantly up-regulated at ZT12 in SP compared to LP, as revealed in the microarray analysis ($p<0.05$) and values were higher at SP's at ZT12 compared to SP's at ZT4 for both *NeuroD1* and *Pbef/Nampt* (2.69 compared to 5.25 and 1.45 compared to 2.25 respectively). Control genes (*18S* and *GAPDH*) did not reveal significantly altered expression in either photoperiod with no significant variation between each condition (ranging from 1 to 1.40 and 0.97 to 1.23 respectively). Radioactive *in situ* hybridization results for sagital and coronal hypothalamic sections collected from sheep kept under SP and culled at ZT3 and ZT11 are shown in Fig. 4. As expected, *Cry1* exhibited markedly altered expression, with low levels at ZT3 (day) and strong induction at ZT11 (night), while *Per1* revealed an opposite pattern of expression with elevated expression at ZT3 (Fig. 4 A, B). Both *Pbef/Nampt* and *NeuroD1* were strongly expressed in the PT (Figs. 4 C, D), and the quantification of the PT revealed that there was significant up-regulation at ZT11 for both transcripts (Fig. 4 E, F). For *NeuroD1*, the pattern of expression was very similar to *Cry1*. *Pbef/Nampt* was also strongly expressed in the PT, but a signal was also observed in the median eminence (ME) (Fig. 5C). In contrast to the PT, quantification of relative changes in expression from ZT3 to ZT11 revealed no significant alterations in *Pbef/Nampt* expression in the ME. *Rorβ* expression in the PT showed a significant down regulation at ZT11 on coronal sections as assessed by *in situ* hybridisation (Fig. 5).

Response of Cry1-assciated genes to acute melatonin treatment

Blood samples from animals treated with melatonin implants (Mélovine®) rose to 131pg/ml melatonin within 30 min of treatment, and were 398 (+/-215), 142 (+/-33) and 301 (+/-156) pg/ml at 1h 30min, 3h 30min and 6h 30min respectively. Un-treated animals had levels of <4 pg/ml. Typical reference samples from animals sampled under natural ambient daytime lighting are <4pg/ml and 260 pg/ml for mid-night. We quantified by *in situ* hybridization genes showing a similar change in expression to *Cry1* at ZT12 (*Cry*1, *Kcnq*5, *NeuroD*1, *Pbef//Nampt* and *Hif1*α; Table S3; Fig. 2). This revealed strong PT expression for all 5 transcripts (Fig. 6). Melatonin treatment resulted in a significant increase in expression for all but *Kcnq5*, with a peak at 3h30min and subsequent decline by 6h30min in all 4 cases. At this latter time point, relative expression levels were still approximately twice that of un-treated control animals, with the exception of *Hif1α*, which had returned to a similar level to that of controls. With the exception of *Nampt*, expression was confined to the PT for all transcripts.

Discussion

Use of cDNA array to identify candidate genes and pathways

In our study, exposure of sheep to LP resulted in a robust activation of prolactin secretion over a two-month period, which was reversed by

exposure to SP consistent with earlier publications on this species (8), providing a key physiological endpoint validating subsequent analyses of the PT for transcriptome analysis. The array we used provided extensive genome coverage (~50%), and because sheep PT tissue provided sufficient material from individual animals to be run on a single array slide, errors associated with RNA pooling were reduced and confidence in the statistical power of the data greatly increased. Our data presented here demonstrates that we are able to use a bovine-derived cDNA array to identify altered expression in ovine genes from the PT. Specifically, the sequence homology with bovine genes was more than 97%, allowing a high level of cross-hybridization (further details in the supplementary information). Further, candidate genes were confirmed by Q-PCR and *in situ* hybridization and in all cases, we identified the correct ovine homologue expressed within the PT (i.e. there were no false positive). We identified 53 to 65% of genes on the array which were expressed in the PT, and this is within the typical range of expression observed in a particular tissue (22). Thus, use of this well characterised cDNA array and sheep PT model offers an excellent insight into global transcriptome changes at a melatonin target site.

Genes exhibiting "time-of-day" alteration in expression

Of all of the genes exhibiting differential expression on the array, the circadian clock regulator *Cry1* exhibited the greatest relative expression change. The relative phasing of arrayed *Cry1* and *Bmal1* clock genes revealed that *Cry1* was strongly down regulated at ZT12 (SP early night induced) with *Bmal1* induced at late night (ZT20) in SP. Our *in situ* hybridisation studies also confirmed that strong expression of *Per1* and *Cry1* were anchored to dawn and dusk respectively, matching the putative offset and onset of the melatonin signal. Collectively, these data are in accord with previous studies of clock gene expression in the PT of sheep and seasonal rodents which show strong phasic expression associated with the rise and fall of the daily melatonin signal (23, 24). Other clock transcripts such as *Hif1α/MOP1*, *GSK3β* and *Rorβ* were also identified as significantly altered in expression on the array, and the subsequent pathway analysis revealed a significant general over-representation of circadian genes within this data set.

Our Q-PCR and *in situ* hybridisation validation revealed that *Pbef/Nampt*, and *NeuroD1* exhibited specific expression in the sheep PT and were strongly expressed at ZT11 (night phase) compared to ZT3 (light phase) in SP-housed animals, matching array outcomes. In contrast, the *Rorβ in situ* hybridisation revealed down regulation at ZT11, also consistent with the array data. The expression pattern of *NeuroD1* and *Rorβ* in the PT very closely matched that of *Cry1*. In contrast, *Pbef/Nampt* exhibited lower levels of expression in the ME, but expression in this structure did not alter with time of day. *NeuroD1* (Neurogenic differentiation factor 1) is a basic helix-loop-helix transcription factor that binds E-boxes after dimerization with other HLH domain containing proteins (25). It is widely expressed in the vertebrate developing central nervous system and is also expressed in specific areas in the adult brain (cerebellum, hippocampus, PVN and DMN (26-28)). *NeuroD1* is a key transcription factor involved in corticotroph regulation and pancreatic beta-cell differentiation (29, 30) and the knock-out in mice is lethal (30). In the adult, it is strongly expressed in the endocrine cells of pancreas, intestine and pituitary and in these structures is known to regulate insulin, secretin and POMC respectively (25, 26, 31, 32)**.** *NeuroD1* thus plays a central role in both the development and subsequent regulation of multiple endocrine tissues, and our data now suggest that it may play an important additional role in the PT.

Pbef (pre-B-cell colony enhancing factor) was first isolated from peripheral blood lymphocytes and was characterised as a growth factor of B cells precursors by facilitating development of early stage B cells (33). As reviewed by Revollo et al (34), *Pbef* is also known as *Nampt* (nicotinamide phosphoribosyltransferase), as it acts as a key rate limiting enzyme in the NAD salvage cycle of the cell, and more recently as *visfatin*. *Pbef/Nampt* has been associated with the development of obesity and insulin resistance

and type 2 diabetes (35, 36) but it is currently unclear whether it is directly involved in the development of insulin resistance, or indirectly as a marker of inflammatory state (37)**.** The gene is strongly expressed in a circadian rhythmical fashion in adipose tissue in mice , and, as we have observed in the PT, strongly co-associated with *Cry1* (38). Our study shows for the first time that *Pbef/Nampt* is strongly and rhythmically expressed in the PT.

A number of studies have linked the NAD cycle of the cell to circadian clock function. For instance, investigations by McKnight and co-workers have shown close links between energy sensing and the NAD cycle and the regulation of circadian clock genes *Clock* and *NPAS2* in the central nervous system (CNS) (39, 40). A key transcriptional regulator of *Pbef/Nampt* is *Hif1α* a close relative of the circadian clock gene *Bmal1* (41, 42) and we observed that *HIF1α* was also strongly induced on our array in early night, at the same time point as *Pbef/Nampt* (i.e. *Cry1*-associated). Both *Pbef/Nampt* and *Hif1α* are strongly induced both in conditions of hypoxia and cell stress (43). HIF1α protein cooperates with bHLH circadian transcription factors such as CLOCK and BMAL1 allowing cross-talks between hypoxic and circadian pathways (44, 45). Through its action on the NAD/NADH cycle *Pbef/Nampt* is the key enzymatic regulator of a sirtuin gene (*Sirt1*) coding for a NAD-dependent deacetylase with widespread actions on cellular senescence and ageing (reviewed in (46)). *Pbef/Nampt* is thus ideally poised to serve both as a link between circadian timing complexes and, *via* its action on the NAD/NADH cycle, as an energy metabolism sensor, regulating through its action on Sirt1 both genomic (i.e. histone modification) and non-genomic pathways (47).

Melatonin regulation of PT gene expression

Recent studies have shown that circadian clock genes are rhythmically expressed in the PT of seasonally breeding mammals, and also in strains of mice which secrete melatonin (23, 24, 48-51). In seasonal rodents and sheep the circadian clock gene *Per1* is expressed in the PT and is activated in the early morning in direct response to the decline in the nocturnal melatonin signal and altered cAMP signalling. In contrast, the clock gene *Cry1* is rhythmically expressed in the dark phase, co-incident with the onset of pineal melatonin secretion, and in both sheep and hamsters melatonin treatment has been shown to directly induce *Cry1* expression in the PT irrespective of the phase of the light/dark cycle (52). PER and CRY are key components of the feedback loop controlling the master clock in the suprachiasmatic nucleus (SCN). These two proteins are co-incidentally expressed within the SCN and heterodimerise to rhythmically modulate circadian gene transcription *via* E-box motifs on target genes (53). Studies of seasonally breeding sheep have revealed that in contrast to the SCN, within the PT *Per1* and *Cry1* mRNA track the offset and onset respectively of the melatonin signal such that seasonal changes in the duration of the melatonin signal are reflected in an altered phase relationship of these two core clock components. From this, it has been proposed that melatonin-regulated seasonal changes in the phasing of the PER/CRY interval may operate as an internal co-incidence detector, providing a genetic mechanism based on circadian clock genes for the PT to decode the seasonal photoperiodic melatonin signal (9, 54-56) and drive down-stream molecular events via E-box mediated transcription. To date, *Cry*1 is the only gene known to be regulated melatonin.

Our study has confirmed earlier studies which demonstrate that *Cry1* is an acutely melatonin-regulated gene and now identifies additional "*Cry*1-associated" genes in the array. Remarkably, several of these (*Pbef/Nampt*, *Hif1α*, and *NeuroD1*) are, like *Cry1*, also strongly induced by melatonin, and over the same time course. These data now suggest that in addition to *Cry1*, melatonin may regulate a number of down-stream molecular pathways in the PT, although we have no insight yet as to whether these novel melatonin-regulated genes contribute to the photoperiodic response, or simply act as a marker of phase for the onset of melatonin secretion. Little is known of how melatonin may induce such rapid changes in gene expression in a target tissue. Classically, this hormone is thought to act by inhibiting

cAMP signalling pathways (57). The speed of transcriptional response in the PT would mitigate against regulation by de-novo production of an intermediate factor, and it is possible that these responses represent direct transcriptional activation by a melatonin-regulated signalling system. *Cry1* and *NeuroD1* are known to be regulated in a circadian manner by E-box acting transcription factors, and we have recently identified a putative E-box site within the presumptive promoter of *Nampt* (Kim, Dupré, unpublished). However, HIF1a is an E-box acting transcription factor and is not known to be regulated itself *via* an E-box. Since a large number of genes were shown to be significantly expressed on SP at ZT12 and several/many of these may also be melatonin regulated, identification of further melatonin regulated clusters may allow us to define unique transcription factor binding sites within the regulatory elements of these genes, and thus candidate proteins for the immediate down-stream pathways on which melatonin acts.

Phenotypes of the PT

To date, no studies have been undertaken of the transcriptome of the mammalian PT and relatively little is known of the genetic phenotype of these cells. Melatonin receptors are strongly expressed in the PT of seasonal mammals, and studies of Siberian hamsters have revealed that PT secretory granules are more numerous in animals housed under LP (58). The mammalian PT contains three different main cell types, a follicular cell (reviewed in (59, 60), pars distalis (PD) cells of gonadotroph origin (61) which have migrated from the PD to the PT and a third cell type which expresses the beta-subunit for TSH and the common alpha glycoprotein hormone subunit (αGSU). These latter cells are known to co-localise with the melatonin receptor in the rat and European hamster (62, 63). In these TSHβ positive cells, levels of immuno-staining are significantly reduced under short photoperiods and are also sensitive to treatment with melatonin or pinealectomy (64, 65). All three cell types are included in any PT dissection; in addition, it is impossible to avoid inclusion of some material from the ME, including GnRH and other nerve terminals and associated glial cells. Therefore, the tissue screened is heterogeneous and not confined solely to melatonin-receptor expressing cells. A remarkable feature of our data is that with the exception of *Nampt* (which reveals weak ME expression as well as PT), all novel PT transcripts identified from the array revealed strong expression by *in situ* hybridization to be specific to the PT, validating this combined approach as a means for detecting novel PT pathways.

Genes exhibiting photoperiodic alteration in expression

By comparing three different time points over the light dark cycle for LP or SP housed animals we were able to identify differentially expressed genes which exhibited a consistent alteration in expression at all three time-points ("photoperiodic" genes) or were significantly altered in expression at a specific phase ("time-of-day" regulated genes). Clearly, genes in this latter category may also be "photoperiodic" if their general waveform of expression over the 24h cycle is sculpted by photoperiod, but with only three time points assessed, we have adopted the conservative classification of these genes as "time-of-day" regulated. Generally, our data revealed that relatively few transcripts exhibited significant alterations in expression (of the order of <1%). Within the photoperiodic gene-set the most strongly altered transcript encoded the prion protein (*PRNP*). Prion proteins are now recognised as serving important biological functions in both the mammalian CNS and lymphoid tissue (66). Within the CNS, the endogenous prion protein is important in neural development, synaptic transmission and neurite outgrowth, probably by binding to the neural cell adhesion molecule (N-CAM) as a signalling receptor (reviewed in (67). mRNA levels for prion proteins have been shown to be highly rhythmic both in the SCN and throughout the forebrain of rats, and in mice severe disruption of circadian activity and sleep-wake cycles is observed in prion protein-deficient transgenic mice (68). Our data suggest that the prion protein may serve an important role in this melatonin target tissue.

We also observed that the potassium channel coded by *Kcnq5*, not previously identified as

being expressed in the PT, was also strongly LP-repressed. A different clone of the same gene was also detected in the SP early night induced gene set, implying that this gene may fall into the category of a transcript in which expression over the day is regulated by photoperiod. *Kcnq5* was only recently discovered and exhibits a strong expression specifically within the CNS (69). Recent studies have shown that *Kcnq5* is strongly expressed in the arcuate nucleus where it co-localises to NPY and POMC neurones (70). Regulation of the Kcnq family of genes are also known to be important for the regulation of neural plasticity in the hippocampus (71). Thus, Photoperiod-responsive expression of *Prnp* and *Kcnq5*, two transcripts implicated in cellular communication and plasticity suggests that such processes may play an important role in the PT of a seasonal mammal. A number of genes exhibiting significant up-regulation on LP's are associated with histone and non-histone protein regulation, including two methyl-transferases (*SUV39H2*; *PRMT5*).

Homologous structures in birds

A recent paper on Japanese quail has used heterologous chicken arrays to reveal key photoperiodic changes in the basal hypothalamus and PT (72). In this study, the authors defined transcript changes over the first two days following an extreme shift from short (4h light) to long (20h light) photoperiods. In quail, this results in a significant rise in luteinising hormone (LH) by the end of the first long day. Using arrays, Nakao et al (72) were able to detect two genes (*Tshβ* and *Eya3*) which were elevated at the end of the light phase of the first long day in the avian PT, and which thus may act as a signal to the neuroendocrine system of photoperiodic activation. Subsequent studies by this group also revealed that TSHβ acted on ependymal cells to induce expression of Deiodinase 2 (*Dio2*), a thyroid converting enzyme known to be critical to the regulation of the hypothalamic reproductive response in birds and mammals (73). Up-regulation of *Dio2* was also associated with a larger number of transcripts showing altered expression in the hypothalamus on Day 2. This study therefore indicates the central importance of the PT to photoperiodic responsiveness in birds, and also demonstrates that photoperiodic activation is associated with synchronized waves of gene expression which follow a strict temporal pattern. *TSHβ* and the common sub-unit (*αGSU*) as well as *Eya3* were arrayed as transcripts on the cattle microarrays we used. However, none of these genes showed significantly altered expression at either time of day or photoperiod. Our current study was based on a comparison of transcript changes in the PT following chronic (14 weeks) exposure to photoperiods and it is possible that altered TSH signaling represents earlier events in the photoperiodic response. Using *in situ* hybridization, a recent study of sheep has also failed to identify significant changes in *TSH* expression on Day 1 of LP exposure in the sheep PT, although in this study the authors collected samples in the early light phase, rather than later in the day when expression might be expected to be elevated (74). It is however highly likely that birds and mammals use a similar pathway and mechanism, as this recent study (74) has shown that altered *Dio2* expression occurs in ovine ependymal cells, and that these cells are responsive to TSH, as in the study of Japanese quail. It is possible that our own study and others have missed the activation of *TSH* by sampling at the wrong time of day, or that in sheep the latency of response to LP differs from birds. These issues can only be addressed by additional studies over a wider range of time points. While further resolution of the identity of common pathways used by birds and mammals must await more extensive studies, it is likely that the photoperiodic response involves a complex series of gene expression changes, from the initial acute responses to the chronic changes detected here following many weeks to months (reviewed in 75).

In summary, we have identified novel PT-expressed transcripts in the sheep, which reveal significant time-of-day alteration in expression. Several of these genes we now show to be directly regulated by melatonin. Identification of the pathways on which these genes act and the manner in which they are regulated, will offer key insight into how this critical melatonin target site translates a seasonally variant melatonin signal into a neuroendocrine output.

Acknowledgements

Plasmids containing a partial cDNA sequence of ovine *Per1*, *Cry1* and murine *Rorβ* were kindly provided by Drs D. Hazelrigg and P. Barrett. We thank Mark Fell at the ARK-genomics facility, Roslin Institute for bioinformatics support, David Bechtold and Karl-Arne Stokkan for comments on the manuscript; Joan Docherty, Marjorie Thomson and Norah Anderson at the Marshall Building sheep research facility, University of Edinburgh for the animal care, Didier Chesneau, INRA Nouzilly, for the melatonin assays, staff of the INRA-UPEA Nouzilly for animal care and Larisa Logunova for technical assistance in cloning *Hif1a* and *Kcnq5* ovine partial cDNAs. This work was supported by the Biotechnology and Biological Sciences Research Council [grant number BBS/B/08744 to ASIL and JRED] and MRC for financial support and the BBSRC ARK-genomics facility at Roslin.

References

1. **Bartness TJ, Powers JB, Hastings MH, Bittman EL, Goldman BD** 1993 The timed infusion paradigm for melatonin delivery: what has it taught us about the melatonin signal, its reception, and the photoperiodic control of seasonal responses? J Pineal Res. 15:161-190.
2. **Curlewis JD** 1992 Seasonal prolactin secretion and its role in seasonal reproduction: a review. Reprod Fertil Dev. 4:1-23.
3. **Morgan PJ, Williams LM** 1996a The pars tuberalis of the pituitary: a gateway for neuroendocrine output. Rev Reprod 1:153-161.
4. **Graham ES, Webster CA, Hazlerigg DG, Morgan PJ** 2002 Evidence for the biosynthesis of a prolactin-releasing factor from the ovine pars tuberalis, which is distinct from thyrotropin-releasing hormone. Journal of Neuroendocrinology 14:945-954
5. **Morgan PJ, Webster CA, Mercer JG, Ross AW, Hazlerigg DG, MacLean A, Barrett P** 1996b The ovine pars tuberalis secretes a factor(s) that regulates gene expression in both lactotropic and nonlactotropic pituitary cells. Endocrinology 137:4018-4026.
6. **Stirland JA, Johnston JD, Cagampang FRA, Morgan PJ, Castro MG, White MRH, Davis JRE, Loudon ASI** 2001 Photoperiodic regulation of prolactin gene expression in the Syrian hamster by a pars tuberalis-derived factor. Journal of Neuroendocrinology 13:147-157.
7. **Hazlerigg DG, Hastings MH, Morgan PJ** 1996 Production of a prolactin releasing factor by the ovine pars tuberalis. Journal of Neuroendocrinology 8:489-492
8. **Lincoln GA, Clarke IJ** 1994 Photoperiodically-induced cycles in the secretion of prolactin in hypothalamo-pituitary disconnected rams: evidence for translation of the melatonin signal in the pituitary gland. J Neuroendocrinol. 6:251-260.
9. **Lincoln GA, Clarke IJ, Hut RA, Hazlerigg DG** 2006 Characterizing a mammalian circannual pacemaker. Science. 314:1941-1944.
10. **Lincoln GA, Johnston JD, Andersson H, Wagner G, Hazlerigg DG** 2005 Photorefractoriness in mammals: dissociating a seasonal timer from the circadian-based photoperiod response. Endocrinology. 146:3782-3790.
11. **Chemineau P, Malpaux B, Pelletier J, Leboeuf B, Delgadillo JA, Deletang F, Pobel T, Brice G** 1996 Emploi des implants de mélatonine et des traitements photopériodiques pour maîtriser la reproduction saisonnière chez les ovins et les caprins. INRA Prod. Anim 9:46-60
12. **Malpaux B, Daveau A, Maurice F, Gayrard V, Thiery JC** 1993 Short-day effects of melatonin on luteinizing hormone secretion in the ewe: evidence for central sites of action in the mediobasal hypothalamus. Biol Reprod. 48:752-60.
13. **Carr AJ, Johnston JD, Semikhodskii AG, Nolan T, Cagampang FR, Stirland JA, Loudon AS** 2003 Photoperiod differentially regulates circadian oscillators in central and peripheral tissues of the Syrian hamster. Curr Biol. 13:1543-1548.
14. **Grossmann S, Bauer S, Robinson PN, Vingron M** 2007 Improved detection of overrepresentation of Gene-Ontology annotations with parent child analysis. Bioinformatics. 23:3024-31.

15. **Ashburner M, Ball CA, Blake JA, Botstein D, Butler H, Cherry JM, Davis AP, Dolinski K, Dwight SS, Eppig JT, Harris MA, Hill DP, Issel-Tarver L, Kasarskis A, Lewis S, Matese JC, Richardson JE, Ringwald M, Rubin GM, Sherlock G** 2000 Gene ontology: tool for the unification of biology. The Gene Ontology Consortium. Nat Genet. 25:25-9.
16. **Camon E, Magrane M, Barrell D, Lee V, Dimmer E, Maslen J, Binns D, Harte N, Lopez R, Apweiler R** 2004 The Gene Ontology Annotation (GOA) Database: sharing knowledge in Uniprot with Gene Ontology. Nucleic Acids Res. 32:D262-6.
17. **Westfall PH, Young SS** 1993 Resampling-Based Multiple Testing: Examples and Methods for P-Value Adjustment. John Wiley & Sons, New York
18. **Draghici S, Tarca AL, Yu L, Ethier S, Romero R** 2008 KUTE-BASE: storing, downloading and exporting MIAME-compliant microarray experiments in minutes rather than hours. Bioinformatics. 24:738-40. Epub 2007 Nov 17.
19. **Kel AE, Gossling E, Reuter I, Cheremushkin E, Kel-Margoulis OV, Wingender E** 2003 MATCH: A tool for searching transcription factor binding sites in DNA sequences. Nucleic Acids Res. 31:3576-9.
20. **Storey JD, Tibshirani R** 2003 Statistical significance for genomewide studies. Proc Natl Acad Sci U S A. 100:9440-5. Epub 2003 Jul 25.
21. **Kijas JW, Menzies M, Ingham A** 2006 Sequence diversity and rates of molecular evolution between sheep and cattle genes. Anim Genet. 37:171-4.
22. **Su AI, Cooke MP, Ching KA, Hakak Y, Walker JR, Wiltshire T, Orth AP, Vega RG, Sapinoso LM, Moqrich A, Patapoutian A, Hampton GM, Schultz PG, Hogenesch JB** 2002 Large-scale analysis of the human and mouse transcriptomes. Proc Natl Acad Sci U S A. 99:4465-70. Epub 2002 Mar 19.
23. **Lincoln G, Messager S, Andersson H, Hazlerigg D** 2002 Temporal expression of seven clock genes in the suprachiasmatic nucleus and the pars tuberalis of the sheep: Evidence for an internal coincidence timer. Proceedings of the National Academy of Sciences of the United States of America 99:13890-13895.
24. **Johnston JD, Ebling FJP, Hazlerigg DG** 2005 Photoperiod regulates multiple gene expression in the suprachiasmatic nuclei and pars tuberalis of the Siberian hamster (Phodopus sungorus). European Journal of Neuroscience 21:2967-2974.
25. **Naya FJ, Stellrecht CM, Tsai MJ** 1995 Tissue-specific regulation of the insulin gene by a novel basic helix-loop-helix transcription factor. Genes Dev. 9:1009-1019.
26. **Lee JK, Cho JH, Hwang WS, Lee YD, Reu DS, Suh-Kim H** 2000 Expression of neuroD/BETA2 in mitotic and postmitotic neuronal cells during the development of nervous system. Dev Dyn. 217:361-367.
27. **Yokoyama M, Nishi Y, Miyamoto Y, Nakamura M, Akiyama K, Matsubara K, Okubo K** 1996 Molecular cloning of a human neuroD from a neuroblastoma cell line specifically expressed in the fetal brain and adult cerebellum. Brain Res Mol Brain Res. 42:135-139.
28. **Nilaweera KN, Ellis C, Barrett P, Mercer JG, Morgan PJ** 2002 Hypothalamic bHLH transcription factors are novel candidates in the regulation of energy balance. Eur J Neurosci. 15:644-650.
29. **Lamolet B, Poulin G, Chu K, Guillemot F, Tsai MJ, Drouin J** 2004 Tpit-independent function of NeuroD1(BETA2) in pituitary corticotroph differentiation. Mol Endocrinol. 18:995-1003.
30. **Naya FJ, Huang HP, Qiu Y, Mutoh H, DeMayo FJ, Leiter AB, Tsai MJ** 1997 Diabetes, defective pancreatic morphogenesis, and abnormal enteroendocrine differentiation in BETA2/neuroD-deficient mice. Genes Dev. 11:2323-2334.
31. **Mutoh H, Fung BP, Naya FJ, Tsai MJ, Nishitani J, Leiter AB** 1997 The basic helix-loop-helix transcription factor BETA2/NeuroD is expressed in mammalian enteroendocrine cells and activates secretin gene expression. Proc Natl Acad Sci U S A. 94:3560-3564.
32. **Poulin G, Turgeon B, Drouin J** 1997 NeuroD1/beta2 contributes to cell-specific transcription of the proopiomelanocortin gene.

Mol Cell Biol. 17:6673-6682.

33. **Samal B, Sun Y, Stearns G, Xie C, Suggs S, McNiece I** 1994 Cloning and characterization of the cDNA encoding a novel human pre-B-cell colony-enhancing factor. Mol Cell Biol. 14:1431-1437.
34. **Revollo JR, Grimm AA, Imai S** 2007 The regulation of nicotinamide adenine dinucleotide biosynthesis by Nampt/PBEF/visfatin in mammals. Curr Opin Gastroenterol. 23:164-170.
35. **Fukuhara A, Matsuda M, Nishizawa M, Segawa K, Tanaka M, Kishimoto K, Matsuki Y, Murakami M, Ichisaka T, Murakami H, Watanabe E, Takagi T, Akiyoshi M, Ohtsubo T, Kihara S, Yamashita S, Makishima M, Funahashi T, Yamanaka S, Hiramatsu R, Matsuzawa Y, Shimomura I** 2005 Visfatin: a protein secreted by visceral fat that mimics the effects of insulin. Science. 307:426-430.
36. **Chen MP, Chung FM, Chang DM, Tsai JC, Huang HF, Shin SJ, Lee YJ** 2006 Elevated plasma level of visfatin/pre-B cell colony-enhancing factor in patients with type 2 diabetes mellitus. J Clin Endocrinol Metab. 91:295-299.
37. **Oki K, Yamane K, Kamei N, Nojima H, Kohno N** 2007 Circulating visfatin level is correlated with inflammation, but not with insulin resistance. Clin Endocrinol 67:796-800
38. **Ando H, Yanagihara H, Hayashi Y, Obi Y, Tsuruoka S, Takamura T, Kaneko S, Fujimura A** 2005 Rhythmic messenger ribonucleic acid expression of clock genes and adipocytokines in mouse visceral adipose tissue. Endocrinology. 146:5631-5636.
39. **Rutter J, Reick M, Wu LC, McKnight SL** 2001 Regulation of clock and NPAS2 DNA binding by the redox state of NAD cofactors. Science. 293:510-514.
40. **Reick M, Garcia JA, Dudley C, McKnight SL** 2001 NPAS2: an analog of clock operative in the mammalian forebrain. Science. 293:506-509.
41. **Segawa K, Fukuhara A, Hosogai N, Morita K, Okuno Y, Tanaka M, Nakagawa Y, Kihara S, Funahashi T, Komuro R, Matsuda M, Shimomura I** 2006 Visfatin in adipocytes is upregulated by hypoxia through HIF1alpha-dependent mechanism. Biochem Biophys Res Commun. 349:875-882.
42. **Bae SK, Kim SR, Kim JG, Kim JY, Koo TH, Jang HO, Yun I, Yoo MA, Bae MK** 2006 Hypoxic induction of human visfatin gene is directly mediated by hypoxia-inducible factor-1. FEBS Lett. 580:4105-4113.
43. **Brahimi-Horn MC, Pouyssegur J** 2005 The hypoxia-inducible factor and tumor progression along the angiogenic pathway. Int Rev Cytol. 242:157-213.
44. **Hogenesch JB, Gu YZ, Jain S, Bradfield CA** 1998 The basic-helix-loop-helix-PAS orphan MOP3 forms transcriptionally active complexes with circadian and hypoxia factors. Proc Natl Acad Sci U S A. 95:5474-5479.
45. **Ghorbel MT, Coulson JM, Murphy D** 2003 Cross-talk between hypoxic and circadian pathways: cooperative roles for hypoxia-inducible factor 1alpha and CLOCK in transcriptional activation of the vasopressin gene. Mol Cell Neurosci. 22:396-404.
46. **Michan S, Sinclair D** 2007 Sirtuins in mammals: insights into their biological function. Biochem J. 404:1-13.
47. **Yang H, Lavu S, Sinclair DA** 2006 Nampt/PBEF/Visfatin: a regulator of mammalian health and longevity? Exp Gerontol. 41:718-726.
48. **Messager S, Hazlerigg DG, Mercer JG, Morgan PJ** 2000 Photoperiod differentially regulates the expression of Per1 and ICER in the pars tuberalis and the suprachiasmatic nucleus of the Siberian hamster. European Journal of Neuroscience 12:2865-2870.
49. **Johnston JD, Tournier BB, Andersson H, Masson-Pevet M, Lincoln GA, Hazlerigg DG** 2006 Multiple effects of melatonin on rhythmic clock gene expression in the mammalian pars tuberalis. Endocrinology. 147:959-965.
50. **Tournier BB, Dardente H, Simonneaux V, Vivien-Roels B, Pevet P, Masson-Pevet M, Vuillez P** 2007 Seasonal variations of clock gene expression in the suprachiasmatic nuclei and pars tuberalis of the European hamster (Cricetus cricetus). Eur J Neurosci. 25:1529-1536.
51. **Stehle JH, von Gall C, Korf HW** 2002 Organisation of the circadian system in

melatonin-proficient C3H and melatonin-deficient C57BL mice: a comparative investigation. Cell Tissue Res. 309:173-182.

52. **Wagner GC, Johnston JD, Tournier BB, Ebling FJ, Hazlerigg DG** 2007 Melatonin induces gene-specific effects on rhythmic mRNA expression in the pars tuberalis of the Siberian hamster (Phodopus sungorus). Eur J Neurosci. 25:485-90.
53. **Ko CH, Takahashi JS** 2006 Molecular components of the mammalian circadian clock. Hum Mol Genet. 15:R271-7.
54. **Johnston JD, Cagampang FR, Stirland JA, Carr AJ, White MR, Davis JRE, Loudon AS** 2003 Evidence for an endogenous per1- and ICER-independent seasonal timer in the hamster pituitary gland. FASEB 17:810-815.
55. **Hazlerigg DG, Andersson H, Johnston JD, Lincoln G** 2004 Molecular characterization of the long-day response in the soay sheep, a seasonal mammal. Current Biology 14:334-339.
56. **Dupre SM, Loudon AS** 2007 Circannual clocks: annual timers unraveled in sheep. Curr Biol. 17:R216-217.
57. **Barrett P, Morris M, Choi WS, Ross A, Morgan PJ** 1999 Melatonin receptors and signal transduction mechanisms. Biol Signals Recept. 8:6-14.
58. **Merks T, Schulze-Bonhage A, Wittkowski W** 1993 Photoperiod-dependent changes in exocytotic activity in the hypophyseal pars tuberalis of the Djungarian hamster, Phodopus sungorus. Cell Tissue Res. 273:287-291.
59. **Morgan PJ, Williams LM** 1996c The pars tuberalis of the pituitary: a gateway for neuroendocrine output. Rev Reprod. 1:153-161.
60. **Wittkowski W, Bockmann J, Kreutz MR, Bockers TM** 1999 Cell and molecular biology of the pars tuberalis of the pituitary. Int Rev Cytol. 185:157-194.
61. **Bockers TM, Bockmann J, Fauteck JD, Wittkowski W, Sabel BA, Kreutz MR** 1996 Evidence for gene transcription of adenohypophyseal hormones in the ovine pars tuberalis. Neuroendocrinology. 63:16-27.
62. **Klosen P, Bienvenu C, Demarteau O, Dardente H, Guerrero H, Pevet P, Masson-Pevet M** 2002 The mt1 melatonin receptor and RORbeta receptor are co-localized in specific TSH-immunoreactive cells in the pars tuberalis of the rat pituitary. J Histochem Cytochem. 50:1647-1657.
63. **Dardente H, Klosen P, Pevet P, Masson-Pevet M** 2003 MT1 melatonin receptor mRNA expressing cells in the pars tuberalis of the European hamster: effect of photoperiod. J Neuroendocrinol. 15:778-786.
64. **Bockmann J, Bockers TM, Vennemann B, Niklowitz P, Muller J, Wittkowski W, Sabel B, Kreutz MR** 1996 Short photoperiod-dependent down-regulation of thyrotropin-alpha and -beta in hamster pars tuberalis-specific cells is prevented by pinealectomy. Endocrinology. 137:1804-1813.
65. **Bockers TM, Niklowitz P, Bockmann J, Fauteck JD, Wittkowski W, Kreutz MR** 1995 Daily melatonin injections induce cytological changes in pars tuberalis-specific cells similar to short photoperiod. J Neuroendocrinol. 7:607-613.
66. **Hu W, Kieseier B, Frohman E, Eagar TN, Rosenberg RN, Hartung HP, Stuve O** 2008 Prion proteins: physiological functions and role in neurological disorders. J Neurol Sci. 264:1-8.
67. **Hu W, Rosenberg RN, Stuve O** 2007 Prion proteins: a biological role beyond prion diseases. Acta Neurol Scand. 116:75-82.
68. **Tobler I, Gaus SE, Deboer T, Achermann P, Fischer M, Rulicke T, Moser M, Oesch B, McBride PA, Manson JC** 1996 Altered circadian activity rhythms and sleep in mice devoid of prion protein. Nature. 380:639-642.
69. **Schroeder BC, Hechenberger M, Weinreich F, Kubisch C, Jentsch TJ** 2000 KCNQ5, a novel potassium channel broadly expressed in brain, mediates M-type currents. J Biol Chem. 275:24089-95.
70. **Roepke TA, Malyala A, Bosch MA, Kelly MJ, Ronnekleiv OK** 2007 Estrogen regulation of genes important for K+ channel signaling in the arcuate nucleus. Endocrinology. 148:4937-4951.
71. **Williams S, Johnston D** 1988 Muscarinic depression of long-term potentiation in CA3 hippocampal neurons. Science. 242:84-87.
72. **Nakao N, Ono H, Yamamura T, Anraku T, Takagi T, Higashi K, Yasuo S, Katou Y, Kageyama S, Uno Y, Kasukawa T, Iigo M,**

Sharp PJ, Iwasawa A, Suzuki Y, Sugano S, Niimi T, Mizutani M, Namikawa T, Ebihara S, Ueda HR, Yoshimura T 2008 Thyrotrophin in the pars tuberalis triggers photoperiodic response. Nature. 452:317-22.

73. **Bechtold DA, Loudon AS** 2007 Hypothalamic thyroid hormones: mediators of seasonal physiology. Endocrinology. 148:3605-7.

74. **Hanon EA, Lincoln G, Fustin J-M, Dardente H, Masson-Pevet M, Morgan PJ, Hazlerigg D** 2008 Ancestral mechanism signals summer in a photoperiodic mammal. Curr Biol. In Press

75. **Hazlerigg D, Loudon AS** 2008 Seasonal life timers: new insights into ancient mechanisms. Curr Biol. In Press

Table 1: Definition of photoperiodic expression gene sets.
Significant: expression differs (either up or down-regulated) between LP/SP days
Not significant: expression equal on LP/SP days.

Gene set	ZT4	ZT12	ZT20
Early	Not Significant	Significant	Any
Late	Not Significant	Not Significant	Significant
Photoperiodic	Significant	Significant	Significant

Table 2: Pathway analysis
Over representation of pathways within gene sets

Gene set	Pathway Name	Impact Factor	p-value	gamma p-value	Unique Pathway-id
SP early night induced	mTOR signaling pathway	3,15	0,0431	0,179	1:04150
	TGF-beta signaling pathway	3,15	0,0431	0,179	1:04350
SP early night repressed	Cytokine-cytokine receptor interaction	5,94	0,0026	0,018	1:04060
	Neuroactive ligand-receptor interaction	3,80	0,0225	0,108	1:04080
	Complement and coagulation cascades	3,07	0,0464	0,189	1:04610
	Jak-STAT signaling pathway	3,02	0,0487	0,196	1:04630
	Type I diabetes mellitus	2,96	0,0520	0,206	1:04940
	Cell adhesion molecules (CAMs)	2,88	0,0561	0,218	1:04514
SP late night induced	ErbB signaling pathway	5,038	0,00649	0,039	1:04012
	Notch signaling pathway	4,517	0,01092	0,060	1:04330
	Regulation of actin cytoskeleton	4,484	0,01129	0,062	1:04810
	Focal adhesion	3,023	0,04864	0,196	1:04510
	Circadian rhythm	2,799	0,06088	0,231	1:04710
	Olfactory transduction	2,799	0,06088	0,231	1:04740
SP late night repressed	PPAR signaling pathway	3,713	0,0244	0,115	1:03320
LP repressed	Olfactory transduction	3,425	0,03254	0,144	1:04740
LP induced	Insulin signaling pathway	3,57	0,02815	0,129	1:04910

Table 3: Transcription factor binding sites

Over representation of transcription factor binding sites within each gene set.

	Class	Name	Matrix	ratio	q value
SP early night repressed	bHLH	Hand1	M00222	1,40	0,081
	bHLH-ZIP	AP-4	M00005	1,46	0,108
		Spz1	M00446	1,29	0,006
	bHSH	AP-2	M00189	1,35	0,010
		AP-2	M00915	1,19	0,108
	bZIP	CHOP	M00249	1,63	0,108
	CC	ER	M00191	1,53	0,103
		PPARalpha	M00518	1,34	0,067
		VDR	M00444	1,25	0,108
	CH	Sp3	M00665	1,86	0,067
		ZF5	M00333	1,27	0,000
		Zic2	M00449	1,10	0,108
	fork head	FOX factors	M00809	1,37	0,081
	paired	Pax-5	M00144	1,16	0,067
	paired-homeo	Pax-3	M00327	1,37	0,108
		Pax-4	M00378	1,15	0,081
	POU	POU3F2	M00463	1,40	0,108
	runt	PEBP	M00984	1,53	0,108
SP early night induced	ARID	MRF-2	M00454	1,23	0,029
	bZIP	C	M00622	1,27	0,013
	CC	GATA-X	M00203	1,25	0,013
		GATA-4	M00632	1,20	0,054
	CH	YY1	M00793	1,55	0,008
		PLZF	M01075	1,42	0,050
		ZF5	M00333	1,24	0,011
	fork head	FOXJ2	M00423	1,50	0,003
	HMG	SRY	M00160	1,38	0,035
		SOX9	M00410	1,25	0,064
	homeo	Cart-1	M00416	1,61	0,000
		IPF1	M00436	1,40	0,006
		CDP	M00102	1,28	0,003
		HOXA5	M00023	1,23	0,000
		Xvent-1	M00445	1,19	0,000
		Ncx	M00484	1,11	0,035
	MADS	MEF-2	M00232	1,83	0,020
	NK-2	Nkx2-5	M00241	1,36	0,002
	paired-homeo	Pax-6	M00097	1,72	0,043
		Pax-4	M00377	1,52	0,000
		Pax-4	M00380	1,15	0,064
	POU	oct-04	M01125	1,95	0,005
		oct-04	M01124	1,64	0,005
		POU3F2	M00464	1,86	0,013
		Octamer	M00795	1,35	0,009
		oct-01	M00248	1,32	0,063
		oct-01	M00137	1,20	0,001
		oct-01	M00136	1,15	0,064
		Tst-1	M00133	1,20	0,000
		POU3F2	M00463	1,15	0,005
	RING	RUSH-1alpha	M01107	1,37	0,026

	Class	Name	Matrix	ratio	q value
SP late night repressed	bHLH-ZIP	USF	M00796	1,70	0,390
	bZIP	C	M00622	1,80	0,397
	CC	PPARgamma	M00515	2,09	0,390
	homeo	HOXA5	M00023	1,51	0,397
		CDP	M00102	1,29	0,397
SP late night induced	bHLH	Tal-1beta	M00065	1,76	0,170
	CC	PPARgamma	M00515	1,33	0,149
	fork head	FOXJ2	M00423	1,28	0,149
	homeo	CDP	M00102	3,49	0,113
		TGIF	M00418	3,10	0,149
		Crx	M00623	2,12	0,054
	HSF	HSF1	M00146	5,01	0,054
	NK-2	Nkx2-5	M00241	1,21	0,149
	paired-homeo	Pax-4	M00380	1,33	0,170
	POU	Tst-1	M00133	1,51	0,054
		oct-04	M01124	1,24	0,149
	Rel	NF-kappaB	M00774	3,82	0,149
LP induced	CC	VDR	M00966	1,30	0,268
	CH	KAISO	M01119	3,12	0,203
		Egr-1	M00243	1,62	0,268
	homeo	CDP	M00102	3,06	0,203
LP repressed	bZIP	MAF	M00983	3,16	0,209
	fork head	FOXJ2	M00423	1,66	0,046
	homeo	Crx	M00623	2,27	0,156
		MEIS1B	M00421	2,12	0,156
	paired-homeo	Pax-4	M00377	1,35	0,167
	POU	POU3F2	M00463	2,17	0,209
		POU3F2	M00464	1,28	0,209
		Tst-1	M00133	1,55	0,029
		Oct-1	M00137	1,46	0,096
	trp	v-Myb	M00227	3,73	0,156

Figure legends

Figure 1: Blood prolactin concentration in sheep kept under long (LP) and short photoperiod (DP)
Animals were placed under long photoperiod (LP: 16 hours light/8 hours dark) for 14 weeks, half of the cohort was culled throughout the light dark cycle at 3 different Zeitgeber (ZT) times (ZT4, ZT12 and ZT20) and 2 weeks later (dashed line), the remaining animals were transferred to short photoperiod (SP: 8 hours light/16 hours dark) for a further 10 weeks. After 10 weeks animals were culled throughout the light dark cycle at the same time points (ZT4, ZT12 and ZT20). Insert indicates the times of cull for each photoperiod treatment.

Figure 2: Characterisation of a *cry1* co-expression gene cluster induced at ZT12 under short photoperiod
Scatter plots showing Log2 values of the fold change SP/LP for each clone at ZT4 *vs.* ZT12 (A) and ZT20 *vs.* ZT12 (B). *Cry1* shows the strongest down-regulation at ZT12 on both scatter plots together with *c9Orf77*, *NeuroD1*, *Pbef/Nampt* and *GTF2A1*.

Figure 3: Validation of photoperiodic expression of *NeuroD1* and *Pbef/nampt* in the PT.
Relative expression of ovine *NeuroD1* (A), *Pbef/nampt* (B), *18S* (C) and *Gapdh* (D) mRNA by quantitative PCR. The results confirm the microarray data showing a strong down-regulation of *NeuroD1* and *Pbef* in LP compared to SP at ZT12 in the sheep PT. Data are shown as relative to the ZT4 value in LP set at 1. Statistical significance was set at *p<0.05, **p<0.01, ***p<0.001 using one-way ANOVA followed by Bonferroni post-hoc test.

Figure 4*: In situ* hybridization and quantification of *NeuroD1* and *Pbef/Nampt* mRNA expression in the PT of SP-housed sheep
Representative expression of *Cry1* (A), *Per1* (B), *Pbef/nampt* (C) and *NeuroD1* (D) in the sheep hypothalamus at the level of the PT, on sagital and coronal 20µM cryostat sections at ZT3 and ZT11.
NeuroD1 (E) and *Pbef/Nampt* (F) are specifically up-regulated in the sheep PT in the dark phase (ZT11) under SP. Scale bar: 1mm. Statistical significance was set at *p<0.05, **p<0.01, ***p<0.001 using one-way ANOVA followed by Bonferroni post-hoc test.

Figure 5: *In situ* hybridization and quantification of *Rorβ* mRNA expression in the PT of SP-housed sheep.
Representative expression of *Rorβ* (A), in the sheep hypothalamus at the level of the PT, on coronal 20µM cryostat sections at ZT3 and ZT11
Rorβ (B) shows a significant down-regulation in the sheep PT in the dark phase (ZT11) under SP. Scale bar: 1mm. Statistical significance was set at *p<0.05, **p<0.01, ***p<0.001 using one-way ANOVA followed by Bonferroni post-hoc test.

Figure 6: *In situ* hybridization and quantification of *Cry1, Kcnq5, NeuroD1, Pbef/Nampt and Hif1α* mRNA expression in the PT sheep treated or not with melatonin
Representative expression of *Cry1* (A), *Kcnq5* (B), *NeuroD1* (C), *Pbef/nampt* (D) and *Hif1α* (E), in the sheep hypothalamus at the level of the PT, on coronal 20µM cryostat sections after 1h30, 3h30 or 6h30 on melatonin treated (Mel) or untreated animals (Ctl). *Cry1* (A), *NeuroD1* (C), *Pbef/nampt* (D) and *Hif1α* (E) show a significant up-regulation upon melatonin treatment (black bars) in the sheep PT. *Kcnq5* (B) doesn't show any significant change in treated animals (black bars) compared to untreated animals (white bars). Statistical significance was set at *p<0.05, **p<0.01, ***p<0.001 using one-way ANOVA followed by Bonferroni post-hoc test.

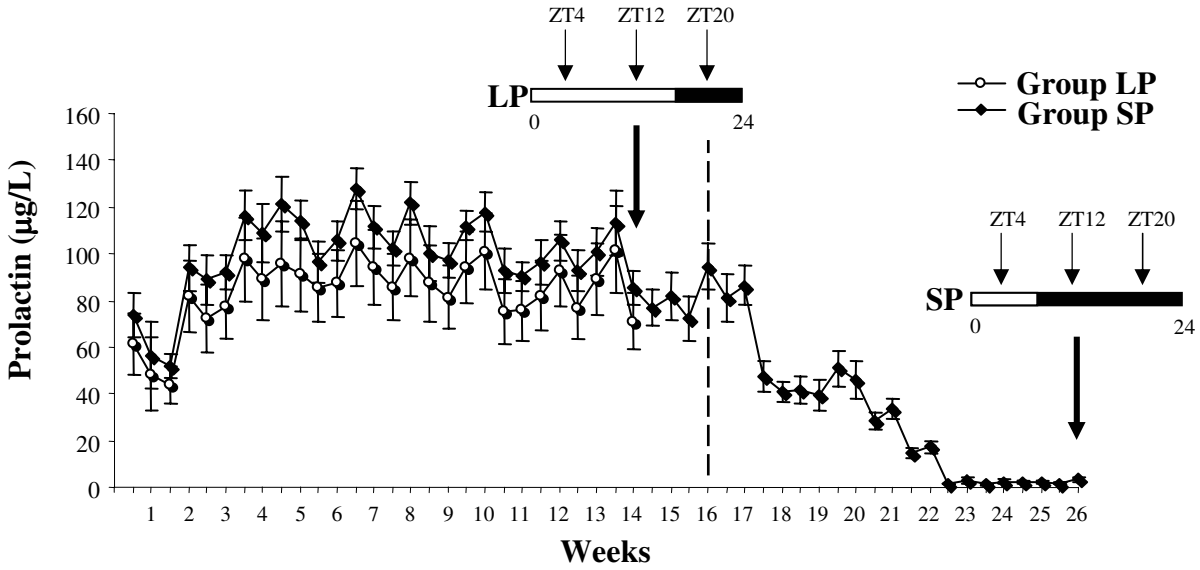
ZT4
ZT12
ZT20
LP
0
24
Group LP
Group SP
ZT4
ZT12
ZT20
SP
0
24
Prolactin (µg/L)
160
140
120
100
80
60
40
20
0
1 2 3 4 5 6 7 8 9 10 11 12 13 14 15 16 17 18 19 20 21 22 23 24 25 26
Weeks

Figure 1

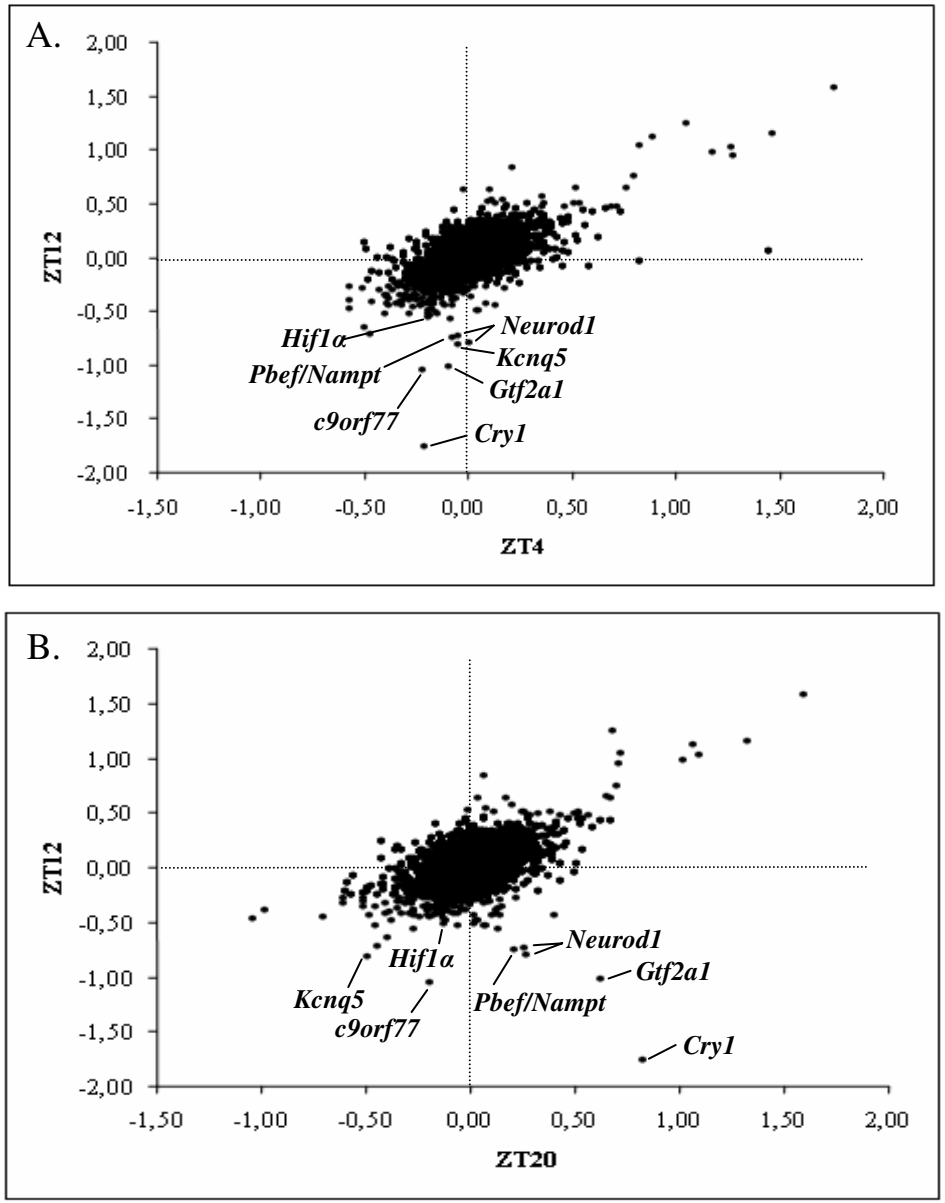
A.
2,00
1,50
1,00
0,50
0,00
-0,50
-1,00
-1,50
-2,00
ZT12
-1,50
-1,00
-0,50
0,00
0,50
1,00
1,50
2,00
ZT4
Hif1α
Neurod1
Kcnq5
Pbef/Nampt
Gtf2a1
c9orf77
Cry1
B.
2,00
1,50
1,00
0,50
0,00
-0,50
-1,00
-1,50
-2,00
ZT12
-1,50
-1,00
-0,50
0,00
0,50
1,00
1,50
2,00
ZT20
Neurod1
Hif1α
Gtf2a1
Kcnq5
Pbef/Nampt
c9orf77
Cry1

Figure 2

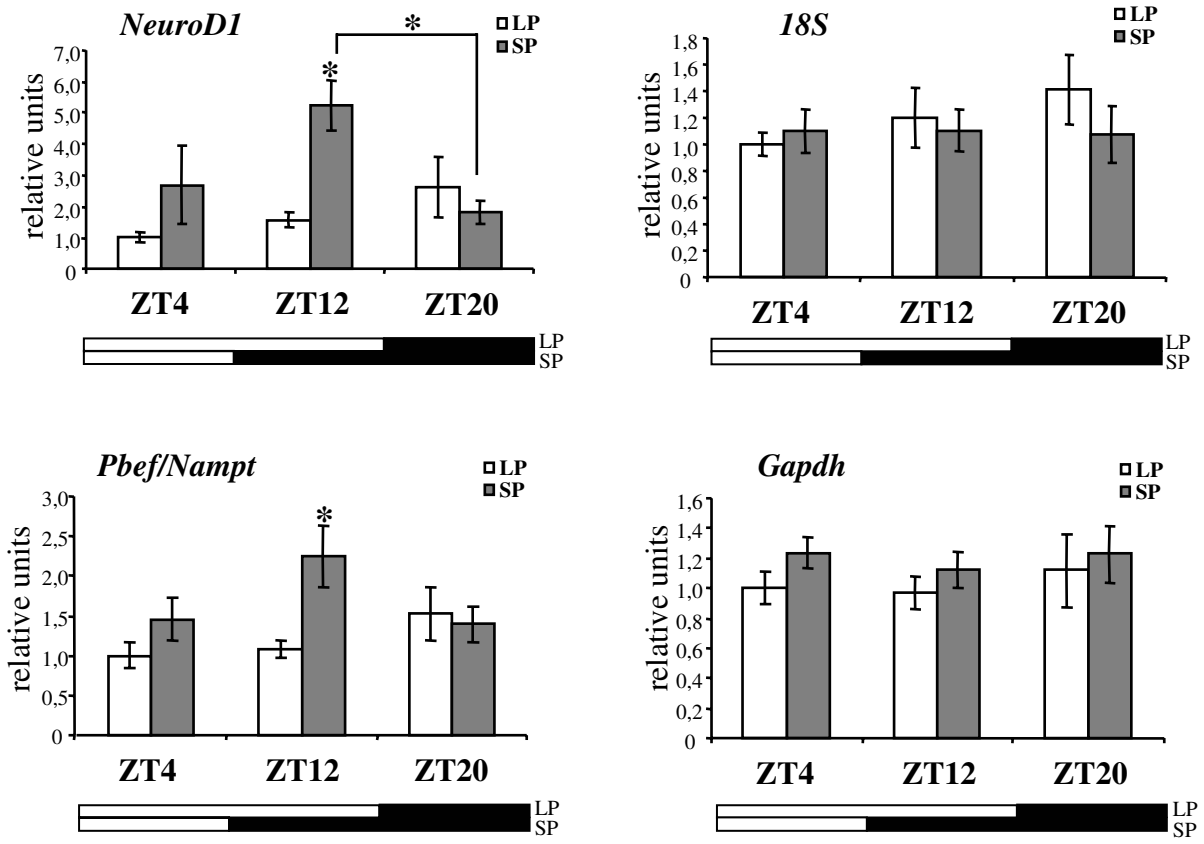
NeuroD1
LP
SP
relative units
7,0
6,0
5,0
4,0
3,0
2,0
1,0
0
ZT4
ZT12
ZT20
LP
SP
18S
LP
SP
relative units
1,8
1,6
1,4
1,2
1,0
0,8
0,6
0,4
0,2
0
ZT4
ZT12
ZT20
LP
SP
Pbef/Nampt
LP
SP
relative units
3,0
2,5
2,0
1,5
1,0
0,5
0
ZT4
ZT12
ZT20
LP
SP
Gapdh
LP
SP
relative units
1,6
1,4
1,2
1,0
0,8
0,6
0,4
0,2
0
ZT4
ZT12
ZT20
LP
SP

Figure 3

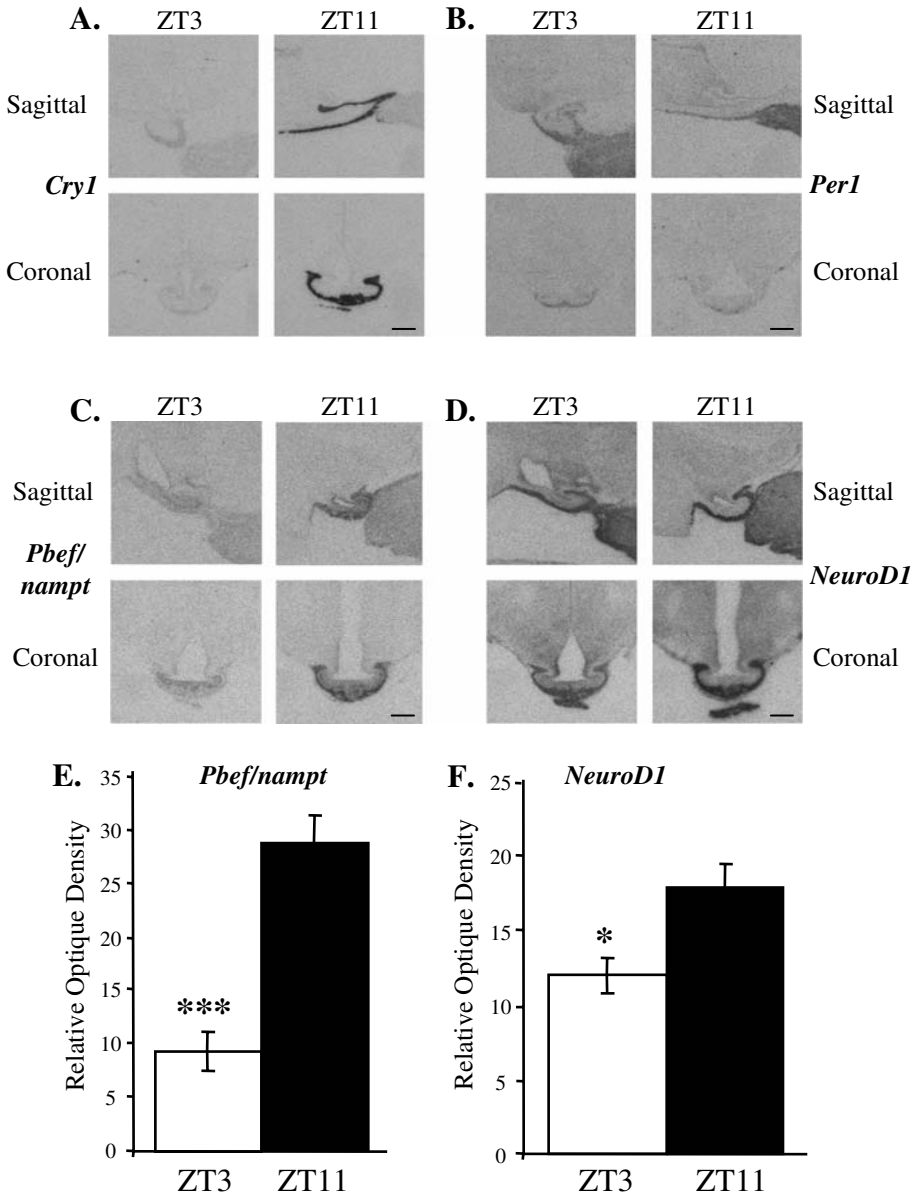
A.
ZT3
ZT11
Sagittal
Cry1
Coronal
B.
ZT3
ZT11
Sagittal
Per1
Coronal
C.
ZT3
ZT11
Sagittal
Pbef/
nampt
Coronal
D.
ZT3
ZT11
Sagittal
NeuroD1
Coronal
E.
Pbef/nampt
Relative Optique Density
35
30
25
20
15
10
5
0
***
ZT3
ZT11
F.
NeuroD1
Relative Optique Density
25
20
15
10
5
0
*
ZT3
ZT11

Figure 4

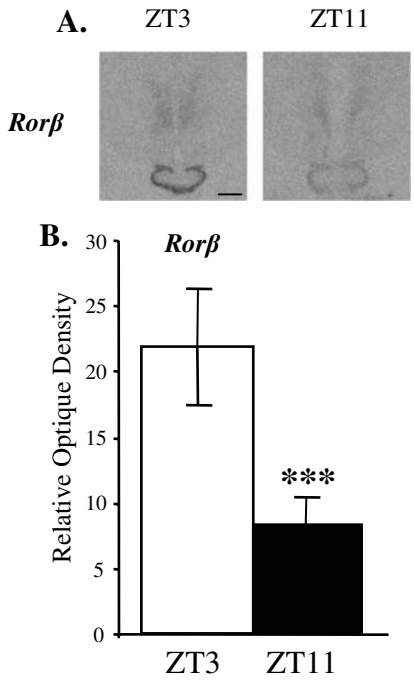
A.
ZT3
ZT11
Rorβ
B.
Rorβ
Relative Optique Density
30
25
20
15
10
5
0
***
ZT3
ZT11

Figure 5

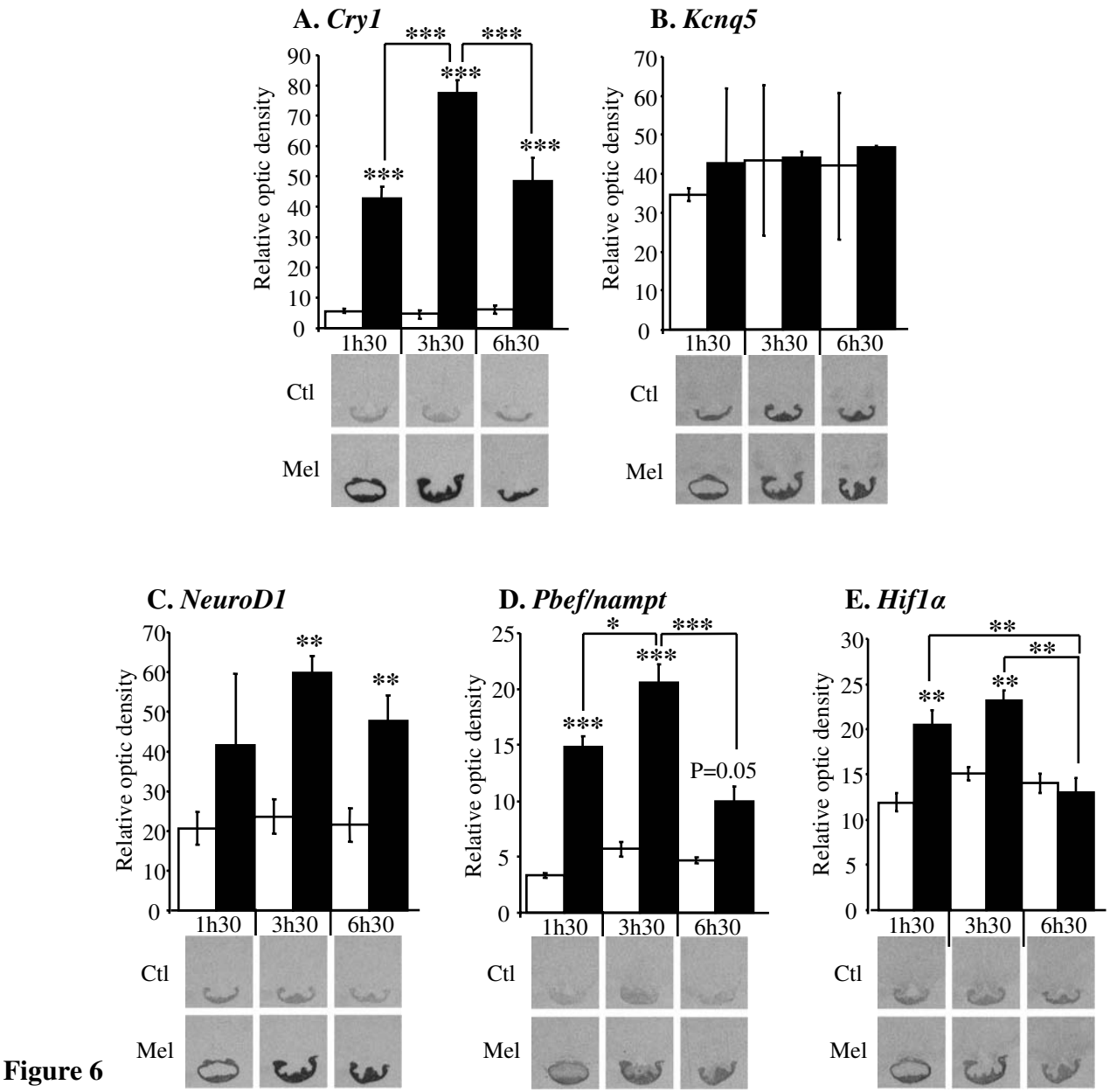
A. Cry1
B. Kcnq5
C. NeuroD1
D. Pbef/nampt
E. Hif1α
Relative optic density
1h30
3h30
6h30
Ctl
Mel
P=0.05

Figure 6